Sains Malaysiana 54(2)(2025): 343-360
http://doi.org/10.17576/jsm-2025-5402-03

Integration of Geophysical Applications in Heterogeneous Near-Subsurface Environments for Archaeological Investigations

(Penyepaduan Aplikasi Geofizik dalam Persekitaran Dekat-Bawah Permukaan Heterogen untuk Penyiasatan Arkeologi)

MUHAMMAD TAQIUDDIN ZAKARIA[1,*], NORDIANA MOHD MUZTAZA[2], ISMAIL AHMAD ABIR[2], NUR AZWIN ISMAIL[2] & SHYEH SAHIBUL KARAMAH MASNAN[3]

[1]*Department of Earth Sciences and Environment, Faculty of Science and Technology, Universiti Kebangsaan Malaysia, 43600 UKM Bangi, Selangor, Malaysia*
[2]*School of Physics, Universiti Sains Malaysia, 11800 USM Penang, Malaysia*
[3]*Centre for Global Archaeological Research, Universiti Sains Malaysia, 11800 USM Penang, Malaysia*

Received: 22 August 2024/Accepted: 7 November 2024

ABSTRACT

Lembah Bujang is well-known for its cultural heritage, comprising a vast variety of archaeological structures and artifacts that could potentially offer valuable insights into the area's historical timeline. However, identifying buried archaeological features via geophysical surveys is a complicated process that necessitates a comprehensive comprehension of both physical properties and archaeological knowledge. To overcome this challenge, a research project was conducted to detect clay brick structures using an integration of geophysical methods such as magnetic and 2-D resistivity at two separate locations within the SB2ZZ and SB2 sites. The research discovered two primary types of archaeological features for these areas, which are mound surfaces and scattered exposed clay bricks. The magnetic data was processed to identify potential clay bricks, which were then confirmed using 2-D resistivity. At the SB2ZZ site, excavations uncovered buried clay brick structures, which reinforced the interpretation of geophysical findings. Both SB2ZZ and SB2 sites demonstrated that clay bricks typically exhibit high magnetic anomalies and resistivity values ranging from 50-140 nT and 400-1000 Ωm, respectively. In conclusion, the combined use of geophysical methods in this study provided detailed subsurface images that were validated by excavation data.

Keywords: Archaeo-geophysics; magnetic; 2-D resistivity

ABSTRAK

Lembah Bujang terkenal dengan warisan budayanya yang terdiri daripada pelbagai jenis struktur arkeologi dan artifak yang berpotensi menawarkan pandangan berharga tentang garis masa sejarah kawasan. Walau bagaimanapun, mengenal pasti ciri arkeologi yang tertanam melalui kajian geofizik adalah proses yang rumit yang memerlukan pemahaman menyeluruh tentang kedua-dua sifat fizikal dan pengetahuan arkeologi. Untuk mengatasi cabaran ini, satu projek penyelidikan telah dijalankan untuk mengesan struktur bata tanah liat dengan menggunakan gabungan kaedah geofizik seperti magnetik dan keberintangan 2-D di dua lokasi berasingan dalam tapak SB2ZZ dan SB2. Penyelidikan tersebut menemui dua jenis utama ciri arkeologi, termasuk permukaan timbunan dan bata tanah liat terdedah yang bertaburan. Data magnetik diproses untuk mengenal pasti bata tanah liat yang berpotensi yang kemudian disahkan menggunakan keberintangan 2-D. Di tapak SB2ZZ, penggalian mendedahkan struktur bata tanah liat yang tertanam, yang mengukuhkan tafsiran penemuan geofizik. Kedua-dua tapak SB2ZZ dan SB2 menunjukkan bahawa bata tanah liat biasanya menunjukkan anomali magnetik tinggi dan nilai keberintangan masing-masing antara 50-140 nT dan 400-1000 Ωm. Kesimpulannya, penggunaan gabungan kaedah geofizik dalam kajian ini memberikan imej bawah permukaan yang terperinci yang disahkan oleh data penggalian.

Kata kunci: Arkeo-geofizik; keberintangan 2-D; magnetik

INTRODUCTION

Lembah Bujang, covering an expansive area of 224 km^2 has gained significant recognition as an archaeological site in Malaysia, offering a wealth of cultural heritage and boasts educational value, dating back to 788 BC (Khaw et al. 2021). The region is home to three prominent archaeological complexes (Figure 1), including Sungai Batu, Sungai Mas, and Pengkalan Bujang, which hold significant archaeological value in terms of chronology, cultural sequence, and periodisation. Among these, Sungai

Batu is the oldest site in Lembah Bujang and has numerous archaeological structures and artifacts that can shed light on the area's history and prehistory, as well as its social and economic context. Previous excavations at Sungai Batu have unearthed clay bricks as the primary construction material. The use of clay/mud bricks has a long history dating back to ancient civilizations, such as Mesopotamia, Egypt, and Rome (Rapi, Jusoh & Saidin 2020), and its analysis has become a crucial aspect of archaeological investigations, as it offers valuable information on sediments, social technology, and cultural knowledge. The prevalence of clay brick distribution in Sungai Batu highlights the society's intellectual stage in architectural knowledge and their ability to manufacture high-quality bricks that are durable, hard, and resistant to natural weathering processes. Such information serves as a marker of chronological and social practice, indicating social class or cultural identity. To fully understand the buried archaeological features in Sungai Batu, geophysical methods such as ground magnetic and 2-D resistivity, were employed. An integrated geophysical approach can provide detailed information on the nature of unseen archaeological targets based on responses to various earth properties (Salvatore et al. 2019). Previous research indicates that the magnetic method has effectively identified brick structures through detecting variations in magnetic properties between the areas of interest and their surroundings, as demonstrated by Ahmed, El Qassas and El Salam (2020) and Pickartz et al. (2019). Similarly, the 2-D resistivity technique has been employed to map the subsurface at various depths by measuring electrical resistivity properties (Akca et al. 2019). In such cases, the role of geophysical surveys over a large area could be decisive in filling the knowledge gap and exploring the buried target at different depths with sufficient resolution. However, detecting buried archaeological features through geophysical surveys is a complex process that requires a thorough understanding of physical properties and archaeological insights. Combining archaeological excavations with geophysical methods offers a comprehensive overview of buried artifacts, structures, and layers, as discussed, either individually or in combined use, in recent publications (Jeon et al. 2022; Milo et al. 2022; Plattner, Filoromo & Blair 2022). The Sungai Batu site is believed to contain buried clay bricks within a silt-clay layer with low physical contrast, and integrated geophysical methods were used to outline the existence and geometry of buried structures in the unexcavated part of the site. This study highlights the significance of clay bricks in the site's architecture and archaeological structures based on a geophysical approach. The main objective of the research was to map archaeological structures in Sungai Batu area with varying sensitivities to geophysical anomalies.

ARCHAEOLOGICAL AND GEOLOGICAL SETTING OF SUNGAI BATU-ANCIENT KEDAH

The discovery of Sungai Batu with systematic excavation in 2009, presents a significant finding in the emergence of the Ancient Kedah. The excavation revealed 54 sites consisting of bricks with various functions, such as iron smelting and monument structures dating back to the 6th century BCE (Mokhtar & Saidin 2018). Previous geophysical work at Sungai Batu has provided insight into the settlement's stratigraphy, which is composed of alluvium (sand, clay, sandy clay), and has shown the presence of an ancient river with a maximum width of 200-300 m, which supports the hypothesis of an early maritime trade industry (Sapiai et al. 2010; Taqiuddin et al. 2017). The archaeological evidence uncovered in Sungai Batu demonstrates the area's role as the polity for primary iron production, including iron mining and smelting activities (Mokhtar et al. 2022). The discovery of furnace segments, iron slag, and tuyeres in smelting areas (1st Century CE), provides important perceptions of the existence of smelting technology and the economic base in this area. A previous study by Saidin et al. (2011) on the paleoenvironment reconstruction of Merbok geomorphology showed that Sungai Batu is the only area of land that was suitable for settlement during the 1st-3rd century CE. Sungai Mas and Pengkalan Bujang remained under the sea or swampy (Figure 1(b)). The findings provide insight into the chronology and periodisation of Ancient Kedah civilisation and also lead to the re-evaluation of the accumulated evidence since the 1840s. The discoveries answered the numerous previous theories regarding the emergence of Ancient Kedah as a port-polity. At least 97 mounds were already mapped, thus reflecting (Figure 1(b)) a great archaeological potential. The discovered ancient smelting furnace and ritual monument embody the significance of early societal involvement in trade and the iron industry, as well as their spiritual adherence. The coastal progradation due to geomorphological factors contributes to the decline of Ancient Kedah as port-polity in the 14th century CE. Sungai Batu became the prominent center for international trade in the 7th century CE, with the discovery of several items of trade and shrines near the Sungai Bujang and Sungai Muda. During 10th-13th century CE, the Ancient Kedah reached its peak of international trade with evidence from the discoveries of Song-Yuan dynasties trade wares. The fluctuation in sea level during the 4th-13th century CE created a more significant land mass (Sungai Mas and Pengkalan Bujang) in the valley with the progradation of the shoreline towards the Strait of Malacca. The shoreline progradation in the Lembah Bujang from the 9th to 13th century CE remained almost similar, except for the changes in the channel flow of the Muda River

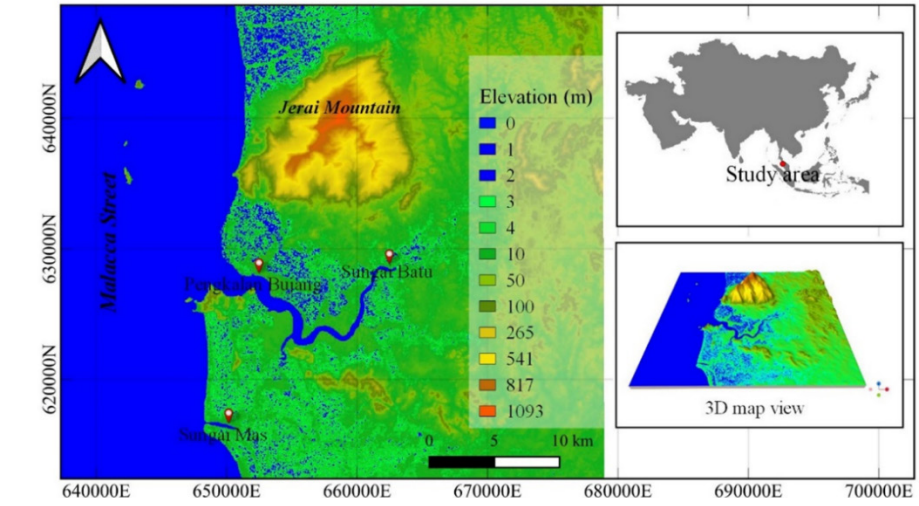

(a)

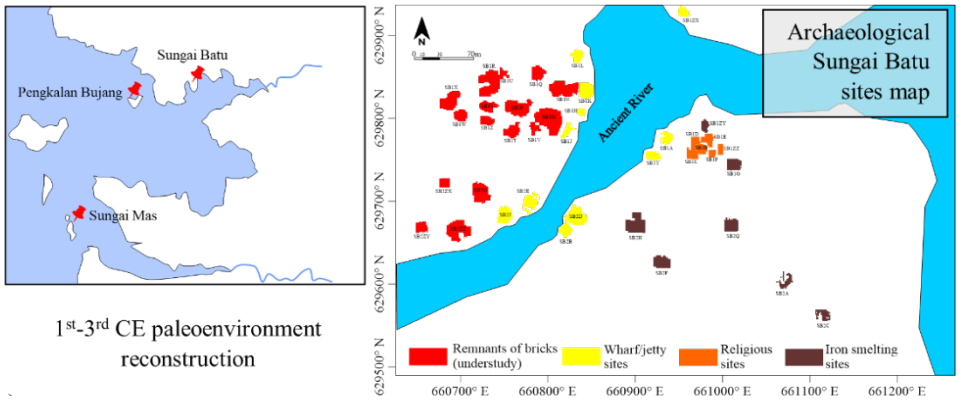

(b)

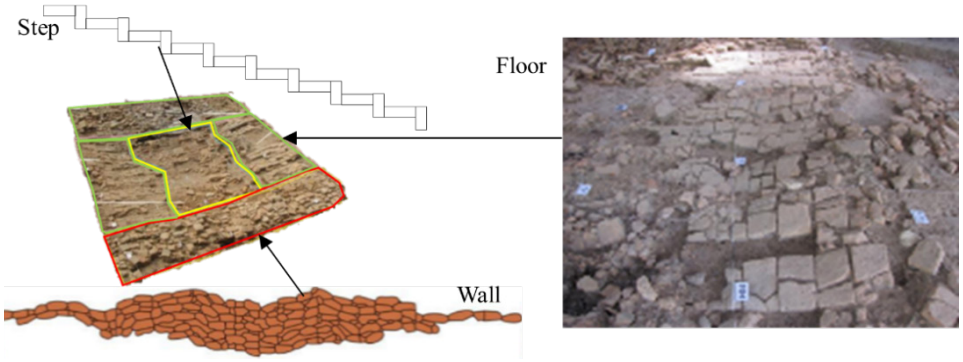

(c)

FIGURE 1. a) Digital elevation model of Sungai Batu area (Shuttle Radar Topography Mission (SRTM)-30 m data modified from USGS Earth Explorer, 2022), b) Paleoenvironment reconstruction of Lembah Bujang during 1st-3rd century CE (modified from Saidin et al. 2011) and the existing archaeological sites map of Sungai Batu (modified from Khaw et al. 2021); c) Jetty structures found in SB2B site includes the step, floor, and wall from clay brick (modified from Zakaria, Saidin & Abdullah 2011)

(Figure 2). However, extreme climate changes during the 14th-15th century CE caused fluctuations in sea level, resulting in the deposition of sediment onshore (Khaw et al. 2019). These changes in the geomorphology of the area affected the activities and functions of Sungai Batu port-polity due to the accessibility of trading vessels in a narrow and shallow bay, leading to a decline in trading activities in the Lembah Bujang and a corresponding regression of Ancient Kedah.

The study areas of Sungai Batu in Kedah are located in the Lembah Bujang territory. It is drained by two principal rivers: Sungai Merbok and Sungai Muda. Gunung Jerai the highest landform in the area, is made of granite (western region), and the rest of the area is covered with sedimentary rocks comprise sandstone/metasandstone with subordinate siltstone, shale, and minor conglomerate. The river channel (Sungai Bujang) starts from the granite area (high slope) and flows down the slope crossing the sedimentary rocks (sandstone/metasandstone with subordinate siltstone, shale and minor conglomerate). The Sungai Batu area is mainly composed of sandy clay covered with fine sand. The geomorphology of the Sungai Batu area is mainly flat with oil palm and rubber tree fields, and also covered with a small stream, rivers, and swampy area in the eastern part of the study area. Geophysical methods of ground magnetic and 2-D resistivity were implemented at two different archaeological sites located about 30 m far from each other. The area is chosen based on the archaeological potential where the surface features of clay bricks are exposed with mound topography.

MATERIALS AND METHODS

DATA ACQUISITION

The Sungai Batu archaeological site has been previously excavated and observed, revealing the remains of floors, pottery fragments, beads, stone tools, and iron slags (Zakaria, Saidin & Abdullah 2011). SB2B was found to have foundations that functioned as a jetty, dating back to the 5th century CE (Figure 1(c)). The architecture of the jetty is characterized by four main features: the wall, floor, step, and roof, with brick being the primary building material in various sizes (Zakaria, Saidin & Abdullah 2011). These brick structures are considered significant features in geophysical mapping. The primary objective of this study was to identify the surface remnants that indicate buried structures through geophysical anomalies. Figure 3 shows the survey map for both study areas of SB2 and SB2ZZ. The geophysical surveys of magnetic and 2-D resistivity methods were conducted at this study areas. SB2ZZ consists of 15 survey lines with a length of 30 m and interval lines of 2 m whereas SB2 consists of 8 survey lines with a length of 20 m and an interval line of 3 m.

The ground magnetic with fixed-base technique was utilised to measure the orientation of Earth's magnetic field intensity and magnitude at a specific location (Won & Huang 2004). Two proton precession magnetometer device was utilised and set at magnetic inter-station distances (rovers) of 1 m with an interval time measurement of 60 s for the base station. The magnetic data was corrected using Microsoft Excel, while Oasis Montaj (ver 7.0) was employed for data imaging and processing. 2-D resistivity method employed direct current to investigate the electrical properties of the subsurface layers. The data was acquired using ABEM SAS4000 system installed with a Pole-dipole array set at a 0.75 m minimum of electrode spacing. The resistivity of earth materials is controlled by their composition, porosity, fluid saturation, and fluid chemistry (Table 1).

Magnetic and resistivity methods offer unique and complementary insights into subsurface features. Fired clay bricks, for instance, exhibit high magnetic susceptibility due to their mineral content and exposure to heat. When these materials cool after firing, they acquire a thermoremanent magnetization (TRM), creating detectable magnetic anomalies (Hervé et al. 2019). The magnetic method is particularly well-suited to detect such anomalies, making

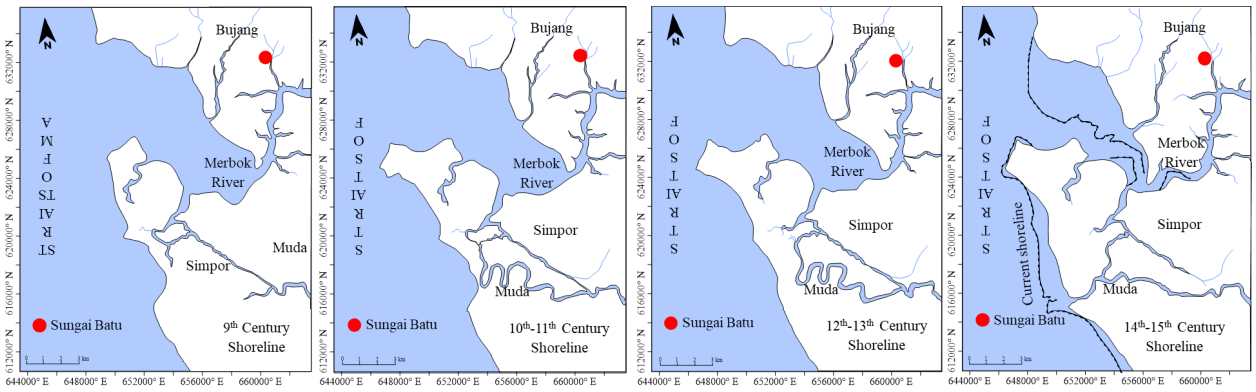

FIGURE 2. Shoreline progradation evolution in Lembah Bujang from 9th - 15th century C (modified from Allen 2000)

TABLE 1. Acquisition setting of the geophysical methods for Sungai Batu survey area

Ground magnetic	2-D resistivity
Rovers	Current maximum: 20 mA
Reading cycle: 3 cycles	Current minimum: 1 mA
Survey type: Gridding mode	Acquisition delay: 0.1 s
GPS: Off	Acquisition time: 0.1 s
	Total time cycle: 1.4 s
Base	Stack Max: 1
Cycle time: 60 s	Stack Min: 1
	Type of array: Pole-dipole

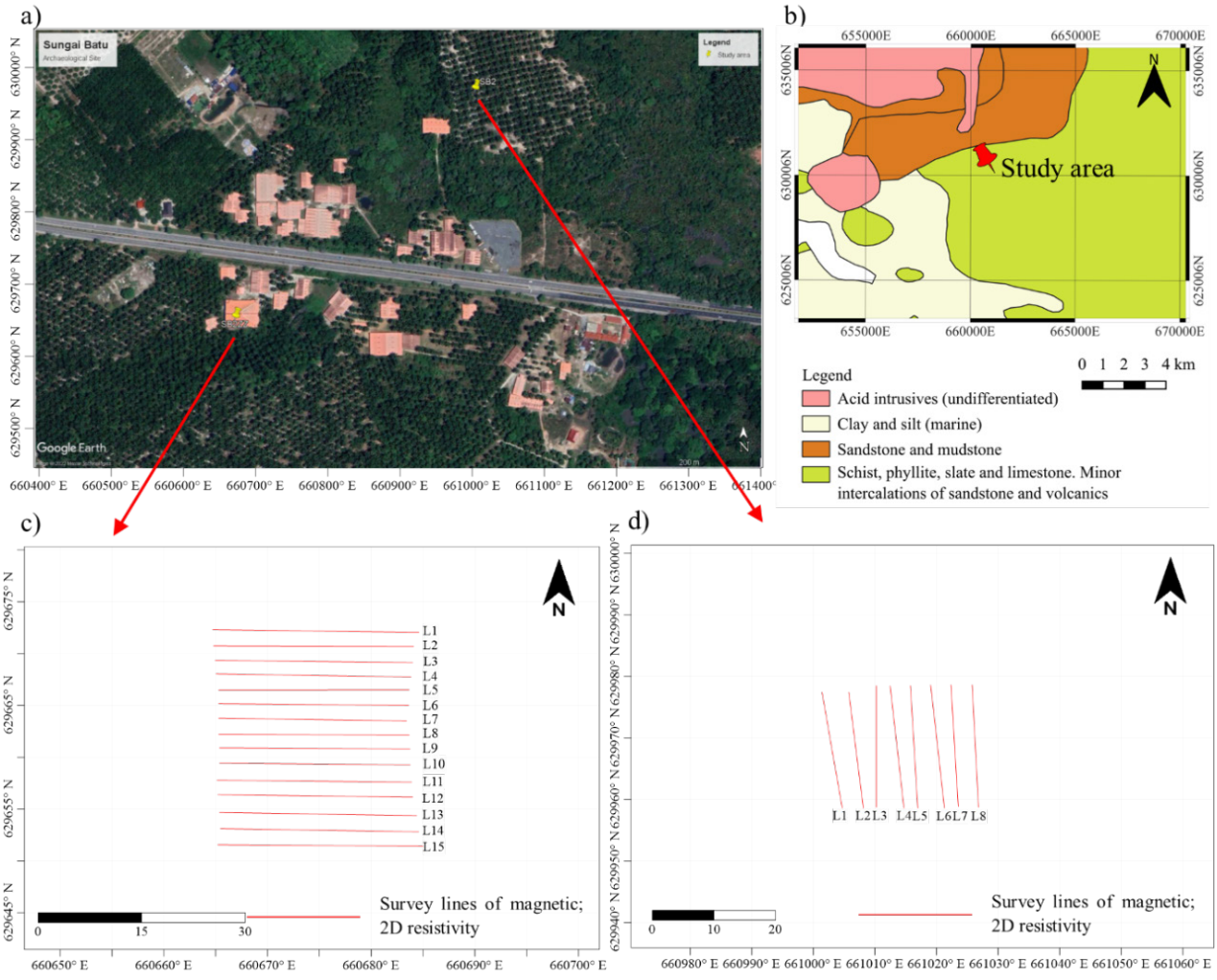

FIGURE 3. Layout study area of Sungai Batu a) Google images show the location of archaeological sites, b) General geology of the study area, c) Geophysical survey layout of SB2ZZ, and d) Geophysical survey layout of SB2

it effective for identifying brick or tile structures and other materials that either naturally contain magnetic properties or have been magnetized through human activities, like heating. In contrast, electrical resistivity measures changes in the ground's conductivity, influenced by factors such as soil moisture, porosity, and the presence of conductive or resistive materials. Archaeological features such as walls, foundations, ditches, and buried structures have distinct resistivity signatures, as they alter the natural distribution of soil moisture and porosity. While magnetic methods excel at identifying fired or metallic objects and large, uniform features, they may overlook non-magnetic or less magnetically distinct structures. Resistivity, meanwhile, detects features with different moisture content more effectively, capturing details magnetic methods may overlook. Using magnetic and resistivity surveys together gives a clearer and more detailed view of a site, with magnetic surveys providing fast preliminary insights and resistivity refining those results.

DATA PROCESSING AND VISUALISATIONS

The ground magnetic data was processed with Oasis Montaj (ver 7) which undergoes several steps of processing to increase the signal-to-noise ratio. The secular and diurnal variation of the magnetic anomaly was removed to generate a magnetic map anomaly as the regional-residual separation was implemented. The processing continues with the horizontal derivative, vertical derivative and analytic signal by using magmap features, whereas the depth analysis is determined from Euler deconvolution included in the software package. The horizontal derivative of the X and Y direction was applied to measure the magnetic field (T) data after removing the diurnal effect to resolve the composite and complex anomalies. The derivatives were able to define the edges of the anomalies, especially for the striking anomalies at a near-perpendicular angle to the direction of the applied derivative (Ansari & Alamdar 2011). The vertical derivative of the Z direction applies to enhance the buried shallow features. The calculated derivatives were then used to measure the analytic signal to determine the location of the causative source of the anomaly. The procedure was extended to derive the depth of the magnetic source using the standard Euler deconvolution, where the technique depends on Euler's homogeneity equation (Equation 1).

$$(x - x_0)\frac{\partial T}{\partial x} + (y - y_0)\frac{\partial T}{\partial y} + (z - z_0)\frac{\partial T}{\partial z} = N(B - T) \quad (1)$$

where (x_0, y_0, z_0) is the location of the magnetic source, the total field is observed at (x,y,z), and $\frac{\partial T}{\partial x}$, $\frac{\partial T}{\partial y}$, and $\frac{\partial T}{\partial z}$ are the derivatives of the magnetic field in the x, y, and z directions, respectively, *B* refers to the regional value of the total field. The homogeneity degree, *N* is constructed as a structure index; where spherical bodies = 3; vertical rod or horizontal cylinder = 2; dike and sill-like structures = 1; and contact equals = 0.5.

Res2Dinv software (ver.3.56.70) was implemented in the inversion process to generate a 2-D resistivity inversion model. The processed and filtered data were then inverted using the smoothness-constrained least-square method (L2-norm) as presented in Equation (2).

$$(\mathrm{J^T J} + \lambda \mathrm{F})\Delta \mathrm{q_k} = \mathrm{J^T g} - \lambda \mathrm{F q_k} \quad (2)$$

where $\mathrm{F} = a_x \mathrm{C_x^T C_x} + a_z \mathrm{C_z^T C_z}$
with $\mathrm{C_x}$ is the horizontal roughness filters; $\mathrm{C_z}$ is the vertical roughness filter; J is the Jacobian matrix of partial derivatives; $\mathrm{J^T}$ is the transpose of J; λ is the damping factor; q is the model change vector; and g is the data misfit vector.

The inversion aims to minimise error, which determines the degree of discrepancy between the calculated apparent resistivity values and those of the input model (Yordkayhun 2021). The inversion shows the optimal results, where the subsurface geology exhibits a smooth variation. The calculated apparent resistivity values of the model block were compared with the measured apparent resistivity values and adjusted iteratively until the values of the model were close to an agreement with the measured apparent resistivity values. The low level of noise and superiority of the data quality was manifested by the lower values of the root mean square (RMS) of <10 %. The inversion model produced by the software was subsequently converted to Surfer format for validation, correlation, and interpretation purposes using the Surfer software.

RESULTS AND DISCUSSIONS

SB2ZZ

Magnetic

Prior to analysis, the field data underwent several calculations and correction procedures, including image processing, to enhance the magnetic anomaly of study areas as shown in Figure 4. Results obtained from the magnetic method yielded detailed information regarding the buried remaining structures. The magnetic values ranging from -14.8 nT to 134.5 nT (Figure 4(a)), with the high magnetic values of 50.1 nT to 134.5 nT potentially indicating the distribution of anomaly features in the area. Some anomaly features were identified in the clay brick distribution, which were detected due to their magnetic contrast with the surrounding environment. This survey was conducted by taking into account the presence of magnetic minerals in the buried archaeological objects. Therefore, archaeological structures made of materials with significant magnetic susceptibility contrast, such as

kilns, furnaces, slag blocks, fireplaces, ceramics, bricks, and tiles, can produce varying magnetisation intensities depending on their magnetic properties.

Generally, the map shows two distinct regions of low (<40.9 nT) and high (>40.9 nT) distribution of the anomalies at the western and eastern parts of the map. The magnetic anomaly map (Figure 4(a)) delineated several potential features associated with the archaeological prospect indicated by the black line dashes. The first two are characterised by a low magnetic anomaly with values of -14.8 nT to -3 nT (regions A and B) while the high anomaly is represented by values ranging from 50.1 nT to 134.5 nT (region C-E). High magnetic (region C) values of 61.8 nT to 134.5 nT are predominant in the northern part of the map and elongated to the central and southern parts with moderate-high values of 40.9 nT to 71.2 nT. This region was associated with the geological setting of the locality with the interbedded sandstone/mudstone, and/or highly magnetised material at a shallow depth. Low magnetic values in the western region indicated the alluvium (sand and clay) from lacustrine depositions. This feature of the adjacent region B elongated towards the eastern direction juxtaposed with a moderate-high anomaly of regions D and E. This could be the result of two-parallel buried structure features striking in this direction. However, further processing is required to delineate this feature. The map presents a complex anomaly of the baked clay features when the magnetised body is spatially close to each other. This produced an annihilated anomaly with the presence of a high anomaly in the northern and eastern regions. It is very complex to delineate the superposition of the target anomaly with the surrounding effect. The calculation of horizontal derivatives of X and Y directions (dx and dy) and vertical derivates (dz) are useful in resolving the composite and complex anomalies into their constituents. The horizontal derivatives emphasise the edges of the anomaly, particularly for striking anomalies at a near-perpendicular angle to the direction of the applied derivative (Ansari & Alamdar 2011). The vertical derivative (dz) in the Z-direction enhanced the anomaly of the buried shallow structures. However, this derivative could also improve the surface noise, which is difficult to characterise from the target anomaly.

From the plotted map shown in Figure 4(b) and 4(c) for the horizontal derivative of X and Y directions, the derivative of Y-direction (dy) showed a clear cut-view of the edges of the anomaly striking from the western to eastern (W-E) direction of map. On the contrary, the horizontal derivative of the X-direction (Figure 4(b)) shows uncertain images of anomaly. The map shows an unclear anomaly of the subsurface, as the horizontal derivative of the Y-direction managed to resolve the complex broad anomaly, specifically of the northern part of the map (Figure 4(c)) into its constituents with values ranging from 15.4 to 23.4 nT/m. The map of Figure 4(b) shows a contradictory result, where some features showed incoherent anomalies between low and high values. Hence, the horizontal derivative of the Y-direction (dy) shows more clearly images where the broad anomaly of the C region of the map (Figure 4(a)) is a result of two spatially adjacent anomalies, which might have resulted from buried structures. Several features were parallel to each other (F-H), which could represent the distribution of the clay brick. The regions of F, G, and H depict moderate-high values of 7.1 to 12.7 nT/m, whereas the region of I showed high values of 15.4 to 23.3 nT/m. This region reflects an identical pattern to the C region on the northern part of the map. The relatively continuous anomaly in Figure 4(c) has been cut into a separate closure in the vertical derivative shown in Figure 4(d). The anomaly in Figure 4(d) showed an identical pattern of the anomaly distributed along with the map with the enhancement of regions G, I, and H. This may be the result of the same features but with an eroded/ irregular pattern, which might be close to the ground surface. Notably, some localised anomalies were enhanced in various places on the map. This is caused by the effect of the surface noise which has been enhanced by vertical derivative and targeted shallow features of the clay bricks.

The previously calculated field derivates were utilised to compute the analytic signal amplitude (Equation 1). This technique was applied to enhance the peak over the edges of the buried dipping contact, which is responsible for the anomaly. The technique is commonly used due to its independency with the inclination, declination, remnant magnetisation, and two-dimensional dip in the source. The calculated result of the analytic signal was plotted in Figure 4(e) with values ranging from 0.2 to 50.7 nT/m. Based on the plotted map, several features could be associated with the buried clay bricks with values ranging from 20. 6 to 50.7 nT/m in regions J, K, and L. Regions K and L show clear positive anomaly with significant width associated with the clay brick interpretation. However, the delineation is difficult where the technique applied resulted in broadening the anomaly as resulted in region J where the anomaly becomes more complex. There are also scattered small anomaly closures covering the map. This could be the result of the effect of the surface, or near the surface, or scattered broken clay bricks.

2-D Resistivity

Figure 5(a) presents the inversion models of 2-D resistivity for the SB2ZZ area from zz1-zz15. The results depict the potential for identifying shallow buried archaeological structures. Based on the inversion models, the high resistivity covers at values of >2000 Ωm, the intermediate resistivity value is from 500 to 1000 Ωm, and the lowest resistivity occurs at values < 100 Ωm. Most inversion models of the 2-D resistivity from SB2ZZ reflected resistivity values from 500 to1000 Ωm out the surface which contains a few anomaly spots at depth of ≤1.5 m and a low resistivity value of ≤500 Ωm underlain at the second layer. The potential anomalies were identified at

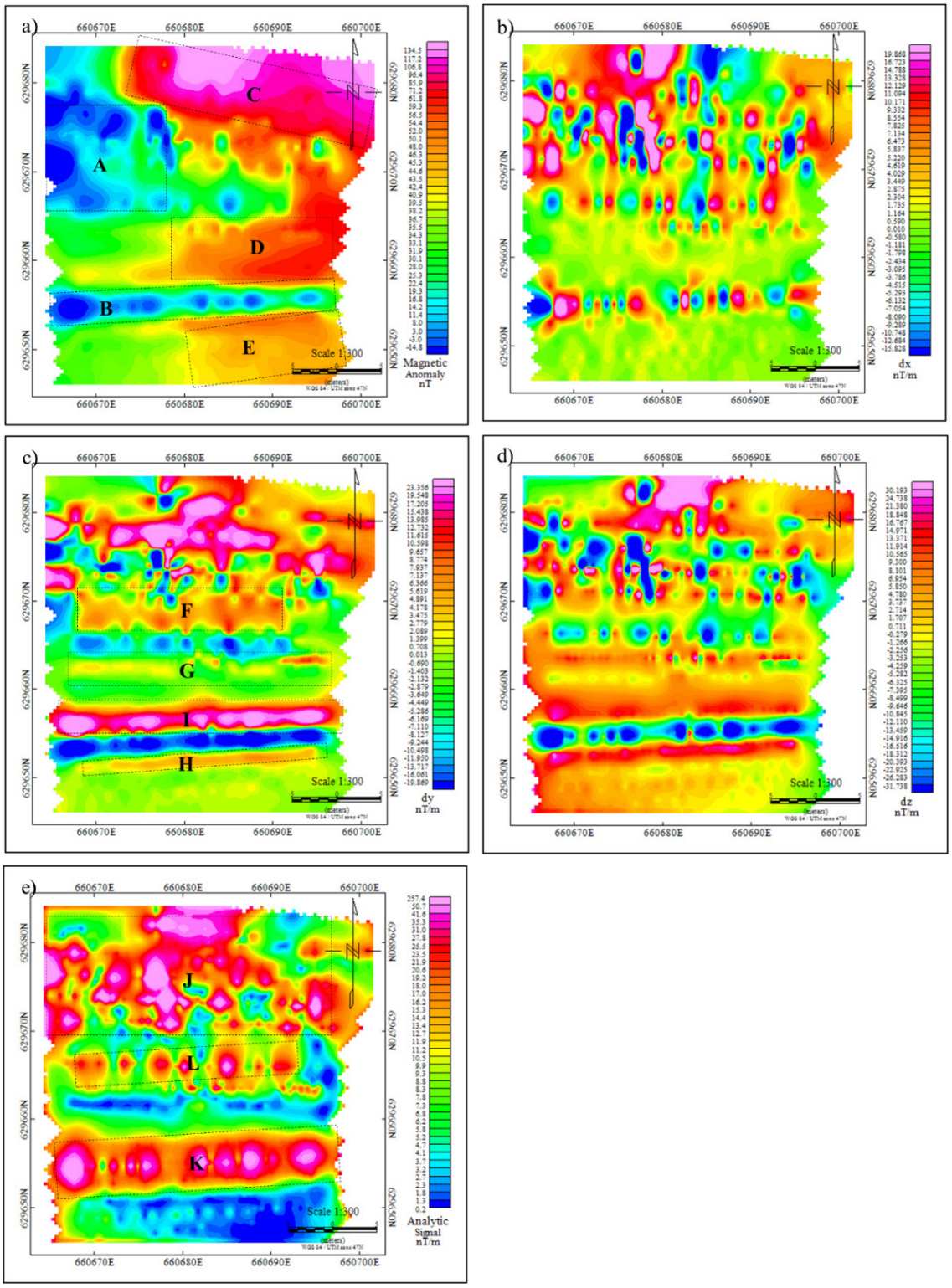

FIGURE 4. Magnetic result of the SB2ZZ, a) Magnetic anomaly, b) Horizontal derivative in the X-direction, c) Horizontal derivative in the Y-direction, d) Vertical derivatives, and e) Analytic signal

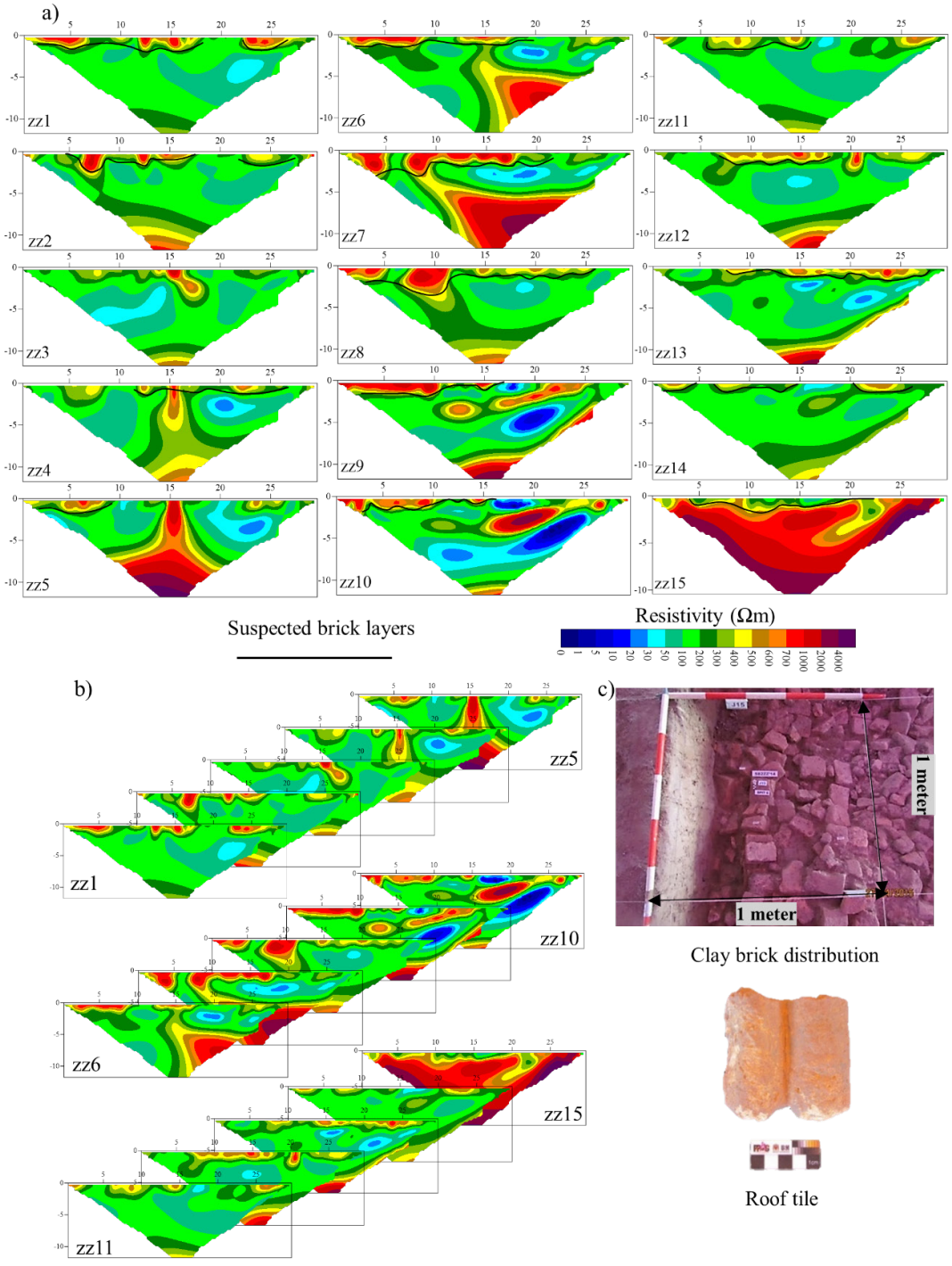

FIGURE 5. a) 2-D resistivity result of SBZZ for line zz1-zz15, b) Orientation of the clay brick anomaly from 2-D resistivity survey lines, and c) Excavated result showing clay bricks distribution and roof tile at SB2ZZ

intermediate resistivity zones at a range from 500 to 1000 Ωm mostly at the top surface at a depth of ≤1.5 m interpreted as possible clay bricks (black solid line). The presence of clay bricks is indicated by high resistivity values due to the extremely strong ceramic bonds formed by the effect of heat at a high temperature. Hardening methods of clay brick manufacture evolved from sun-drying to industrial ovens, which allowed the strength and durability to increase. Bricks could be further dried under the sun, in the open air, which is either designated by sun-dried bricks or put in a kiln with temperatures on the order of 1000 °C where they were fired. Firing allowed the bricks to acquire much more resistance from both mechanical and chemical points of view. Vargemezis et al. (2013) stated that high resistivity values between 123 and 778 Ωm correspond to the building remains, which are mainly located up to a depth of 2.5 m. Figure 5(b) shows the orientation of clay bricks distribution marked with black solid lines at depth <1.5 m. The excavation revealed the buried structures at this locality covered an area of 19 × 19 m^2. Meanwhile, Figure 5(c) presents the *in-situ* floor structures of the clay brick distribution, with the roof tile at the SB2ZZ site. Based on the archaeological result, the findings on the ruins and artifacts found on the SB2ZZ site suggested that it serves as a multi-functional building at the Sungai Batu complex. Due to the large size of the building structures on this site and built towards the ancient river, it is proposed that the site is an important structure in the southern part of Sungai Batu.The region has a low resistivity value that lies within 2 to 5 m, which can be associated with the deposited alluvium composed of sand or sandy clay. The intermediate resistivity could refer to the hard layer underlain by the shale layer of the profile (Taqiuddin et al. 2017).

SB2

Magnetic

Figure 6 illustrates the magnetic result acquired at the SB2 locality with interesting features of archaeology prospects. These features were detected according to the magnetic contrast between the surrounding environment with the clay bricks distribution. The map of Figure 6(a) indicated two different magnetic distributions of the locality with high values zones (region A and C) dominated at the range of 104.4-188.1 nT in the western and eastern regions of the map. Meanwhile, the low magnetic zone (region B) with values of -81.4-1.6 nT dominates at the centre of the map elongating from the northern to the southern region. High values of the magnetic anomaly at regions A and C could represent the clay bricks anomaly, which elongates parallel from the northern to the southern of the map. The high intensities in region C with values of 155.9-188.1 nT could represent the shallow/near-surface buried structures, whereas low magnetic values in region B are associated with sediment deposits. Further detailed assessments are required to examine region C given that it was surrounded by a high magnetic anomaly. The magnetism of a brick is associated with iron-containing clay. Bricks are usually made of kiln-baked mixtures of clay. The heated process produces more magnetic strength compared to the original conditions. The iron minerals in the clay contribute to the good conducting ability of the earth's magnetic field (Bevan 1994). In reference to the magnetic survey conducted by Tong et al. (2013), high magnetic anomalies are associated with the location of the stony ridge and are unlikely to be caused by subsurface archaeological remains.

The horizontal and vertical derivation calculation was applied to resolve the complex anomalies. The horizontal derivative of the X-direction (Figure 6(b)) showed a clear view of the region C anomaly striking from the northern to the southern part of the map. Several features were associated with the identical pattern of the C region parallel to each other, which represents the distribution of clay bricks anomaly. The horizontal Y-derivative show an inconstant pattern with several closures of low and high values distributed along with the map (Figure 6(c)). The X-direction horizontal derivative yielded a more reliable outcome for this locality compared to the Y-direction derivative. This derivative is measured along the actual paths of the surveyed traverses, as the survey conducted is perpendicular to the general azimuth of nearby exposed clay brick. The Y-derivative map failed to enhance the image of these features as the measurement underwent a parallel direction. This enhancement indirectly emphasises the buried structure, which has the same azimuth as the exposed clay bricks. The horizontal X-direction was achieved to resolve the complex anomaly for regions A and C into their components. For example, the broad anomaly of region A (Figure 6(a)) was a result of two spatially adjacent anomalies of regions D and E (Figure 6(b)). Another similar pattern was identified in region F with slightly increased values of 53.8-84.1 nT/m. This identical pattern of regions D, E, and F could represent the anomalies of the buried clay bricks striking from the northern to the southern of the map. The relative continuous anomalies in the X-derivative map have been cut into separate numbers of isolated closures in the vertical derivative map (Figure 6(d)). Several localised anomalies were enhanced in various locations with the surface noises and targeted features. The analytic signal map (Figure 6(e)) showed a similar pattern to the X-derivative map, where high values ranging from 111.2-259.4 nT/m were associated with the distribution of the clay bricks anomalies. However, the previously applied technique could broaden the anomaly. Notably, several anomaly closures covered the map which probably resulted from scattered broken clay brick.

2D Resistivity

Figure 7 presents the inversion models of 2-D resistivity results at the SB2 area for lines SBL1-SBL8. Commonly, the inversion model showed three different resistivity zones composed of high, intermediate, and lowest with values

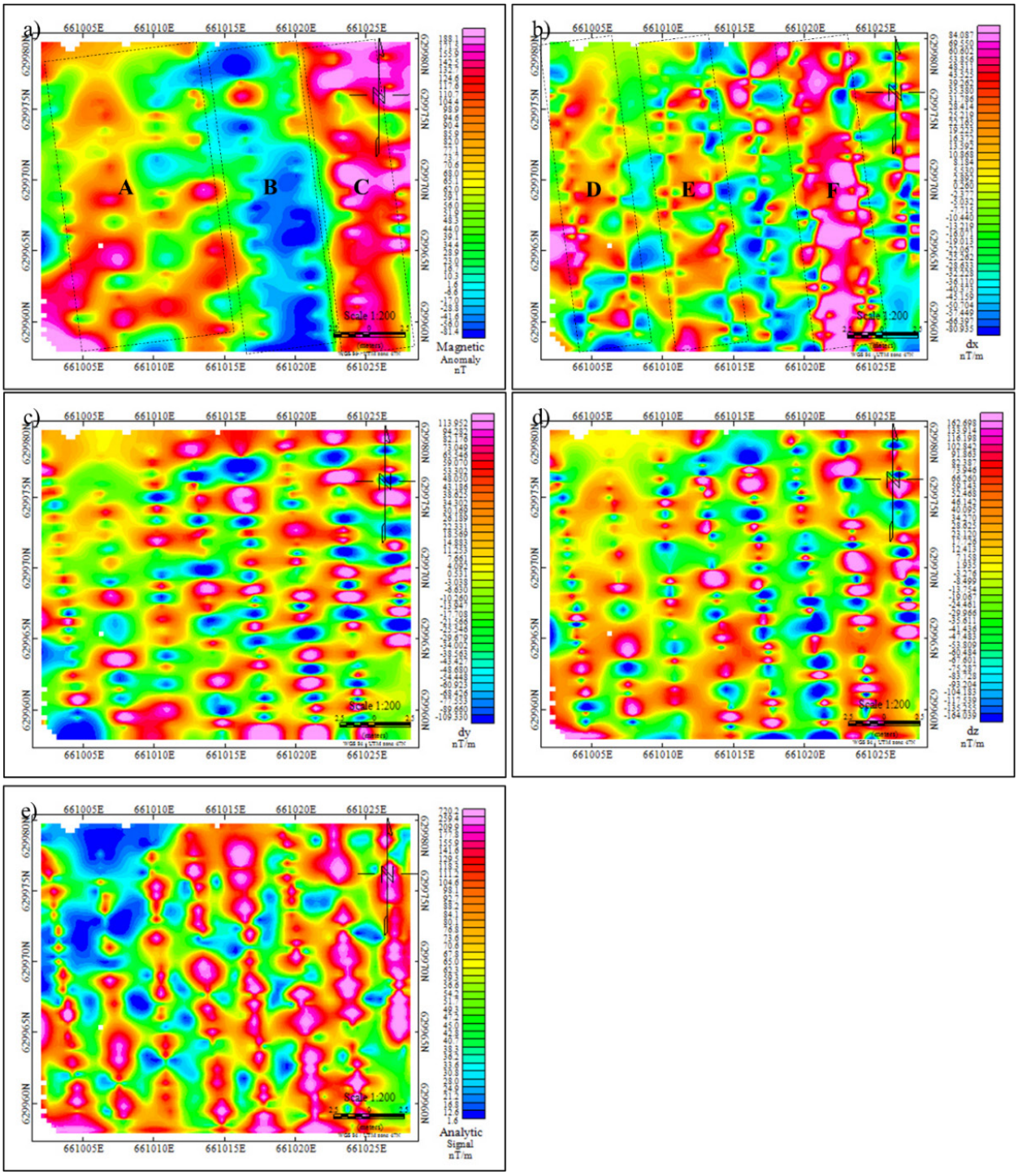

FIGURE 6. Magnetic result of SB2; a) Magnetic anomaly, b) Horizontal derivative in the X-direction, c) Horizontal derivative in the Y-direction, d) Vertical derivatives, and e) Analytic signal

ranging from 800-5000 Ωm, 300-500 Ωm, and <100 Ωm, respectively. Several regular patterns of high resistivity ranges are highlighted with black solid lines at depths <1.5 m that could represent the buried clay brick structures. These features are distributed along the top surface from SBL1-SBL8 with irregular pattern anomaly, which might be due to the presence of brick walls that had collapsed from their original positions. Figure 7(b) and 7(c) depicts the orientation of clay brick anomalies and the exposed clay brick at the top surface of the survey lines. A large distribution pattern at distances of 10-20 m was observed at line SB2L6-SB2L8 as compared to SBL1-SBL5. This region could be associated with the base floor or wall of the archaeological structure. Strong clay bricks with low water absorption and heat resistance produce a hard, dense brick with a smooth shiny face, which probably yields high resistivity values. Vargemezis et al. (2013) conducted a 2-D resistivity survey and suggested that the building's remains reflected high resistivity values. Samsudin and Hamzah (1999) also performed a 2-D resistivity survey and concluded that high resistivity values correspond to the wall of the fort foundation. The lowest range of resistivity (1-300 Ωm) for the locality was mostly distributed at depths >2 m, which probably indicated that the alluvium is composed of sand and sandy clay. A previous study in the nearby area indicated that resistivity values <100 Ωm refer to saturated conditions, which are composed of sand and sandy clay (Taqiuddin et al. 2017). The research showed the lithology of the area which correlated with the borehole record. Generally, the Sungai Batu area was dominated by sand and sandy clay with a maximum depth of up to 25 m, which is considered a large volume of soil deposition. While intermediate resistivity of >500 Ωm at depth >6 m refers to the shale layer with an N-value of 50 to 70 blows (Taqiuddin et al. 2017). Several isolated resistivities of <100 Ωm are seen at depths >2 m, thus indicating the saturated zones. The presence of a small channel nearby of the survey area (Figure 7(d)) probably resulted in the lower resistivity for saturated conditions.

Qualitative Analysis of SB2ZZ and SB2

The analysis of magnetic anomalies was extensively conducted using Euler deconvolution in order to map the lateral location depths of their causative sources. The technique is based on the mathematical approaches for Euler's homogeneity (Equation 2), without resources to any geological constraints (Pánisová & Pašteka 2009; Piro et al. 2007). The benefit of Euler's equation is its independency of magnetic inclination, declination, and remanence, as these factors have become a part of the constant in the anomaly function of a given model (Aziz et al. 2013). Two various approaches were applied to generate solutions for the previous equations: the Standard Euler Deconvolution and Located Euler Deconvolution. The Standard Euler Deconvolution calculates data within a fixed and squared window, where every data point is analysed in a constant grid to produce numerous solutions over the grid. On the other hand, the second approach limits the number of calculations in which the depths are determined at the positions of the field maxima. The positions are located using an analytic signal amplitude (FitzGerald, Reid & McInerney 2004). Both approaches were applied for the magnetic data analysis with a structural index of 1. Figure 9(a) and 9(b) presents the results from both approaches for the SB2ZZ. The standard Euler results (Figure 8(a)) demonstrate more solutions as compared to the located Euler, which was concentrated along a specific trend. These solutions are more likely to be the margin of the buried structures. The standard Euler distinguished more features of suspected clay brick with varying depths of 0.1 to 2.0 m distributed along the map. Notably, more solutions are concentrated in region A (Figure 8(a)) with a horizontal trend covering from the western to the eastern part of the survey, which probably indicates the floor of the structures at depth 1.0-2.0 m. Another similar feature was observed in region B, which is probably a continuous floor structure from region A. The vertical outline at depth 0.5-1.0 m in region B indicated the outer foundation, which probably indicated the collapse of wall structures. Meanwhile, the located Euler demonstrates an insignificant result as the data is limited to the maxima locations.

Figure 8(c) shows the integration of magnetic anomaly with the inversion model of 2-D resistivity for lines zz1 and zz13 of the SB2ZZ area. The magnetic contour map shows the high magnetic value in the range from 50 to 140 nT and the inversion model. Meanwhile, the high resistivity value was in the range of 800 to 5000 Ωm at the top surface and a depth of ≤ 1.5 m, which was associated with the clay bricks at a shallow depth. Based on the observation from the magnetic zz1 line at distances ranging from 11 m to 18 m and 23 m to 29 m, the high magnetic value (50-140 nT) corresponds well with the resistivity zz1 line, which also depicted a high resistivity value (up to 1000 Ωm) at the same distance. Previous research has also demonstrated that high magnetic values of 50-140 nT represent the distribution of the clay bricks (Ihsan et al. 2015). Line zz13 shows the increasing magnetic values from a distance of 14 to 28 m with corresponding resistivity values of 400 to 1000 Ωm. The anomaly elongated towards the east of the map as shown previously in Figure 8(c) for region A, which might be related to the floor of the buried structure. The magnetic trend reflects a gradual pattern towards the east of the map, which represents the distribution of buried clay bricks along the survey line. The resistivity anomalies were mapped at values of 400-1000 Ωm at depths of 0.5 m and 1.2 m. Resultantly, the distribution increases with depth up to 1.223 m, which might as well represent the floor of buried structures. This finding corroborated with the analytical signal map as the distribution of the source was identified at a depth ranging from 0.5-1.2 m (Figure 8(d)). The map showed the edges of the buried structure or clay brick were located on the Euler map. Several closures

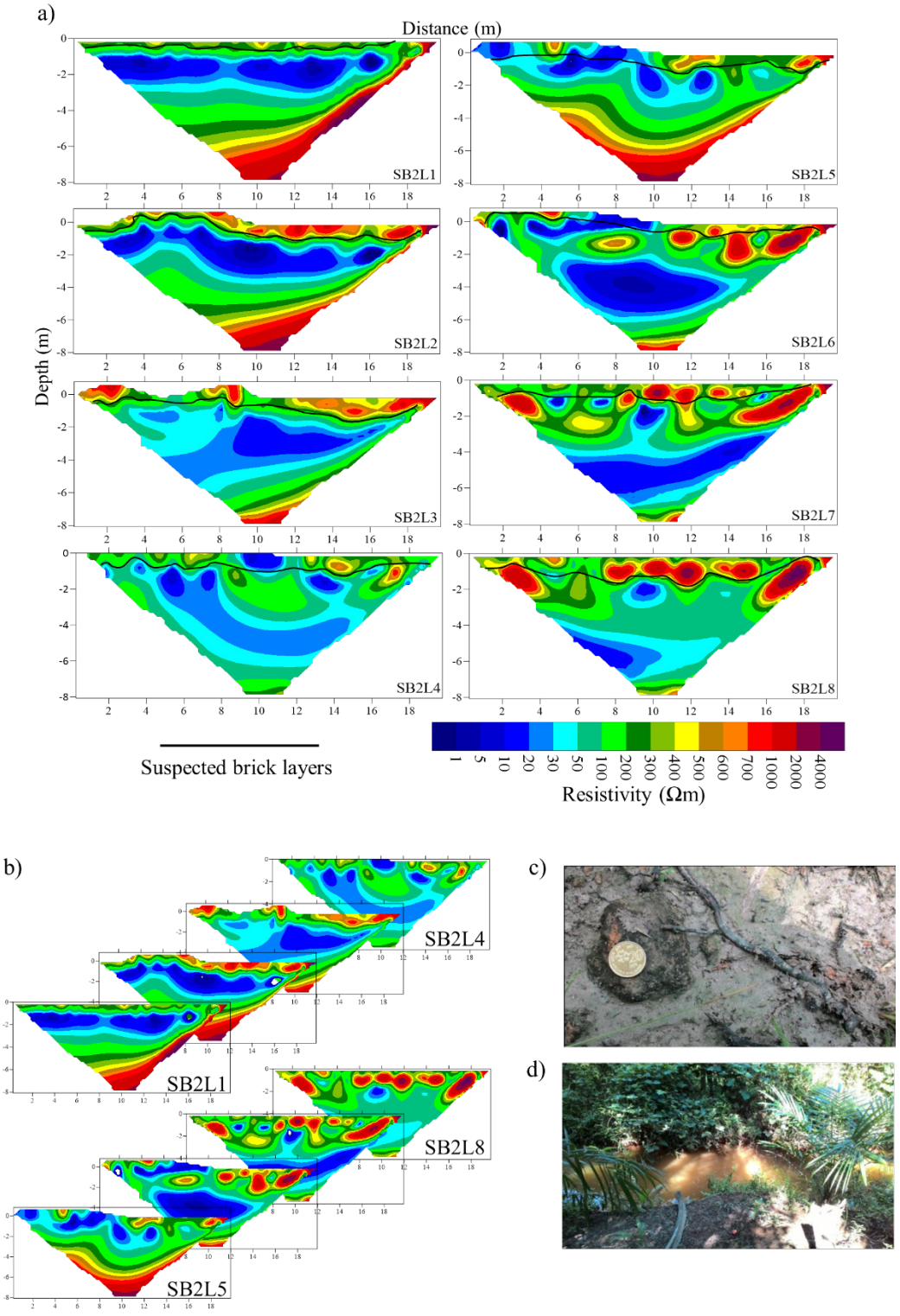

FIGURE 7. a) 2-D resistivity result of SB2 for line SB2L1-SB2L8, b) Orientation of the clay brick anomaly from 2-D resistivity survey lines, c) Exposed clay brick in SB2 survey area, and d) Small channel in SB2 survey area

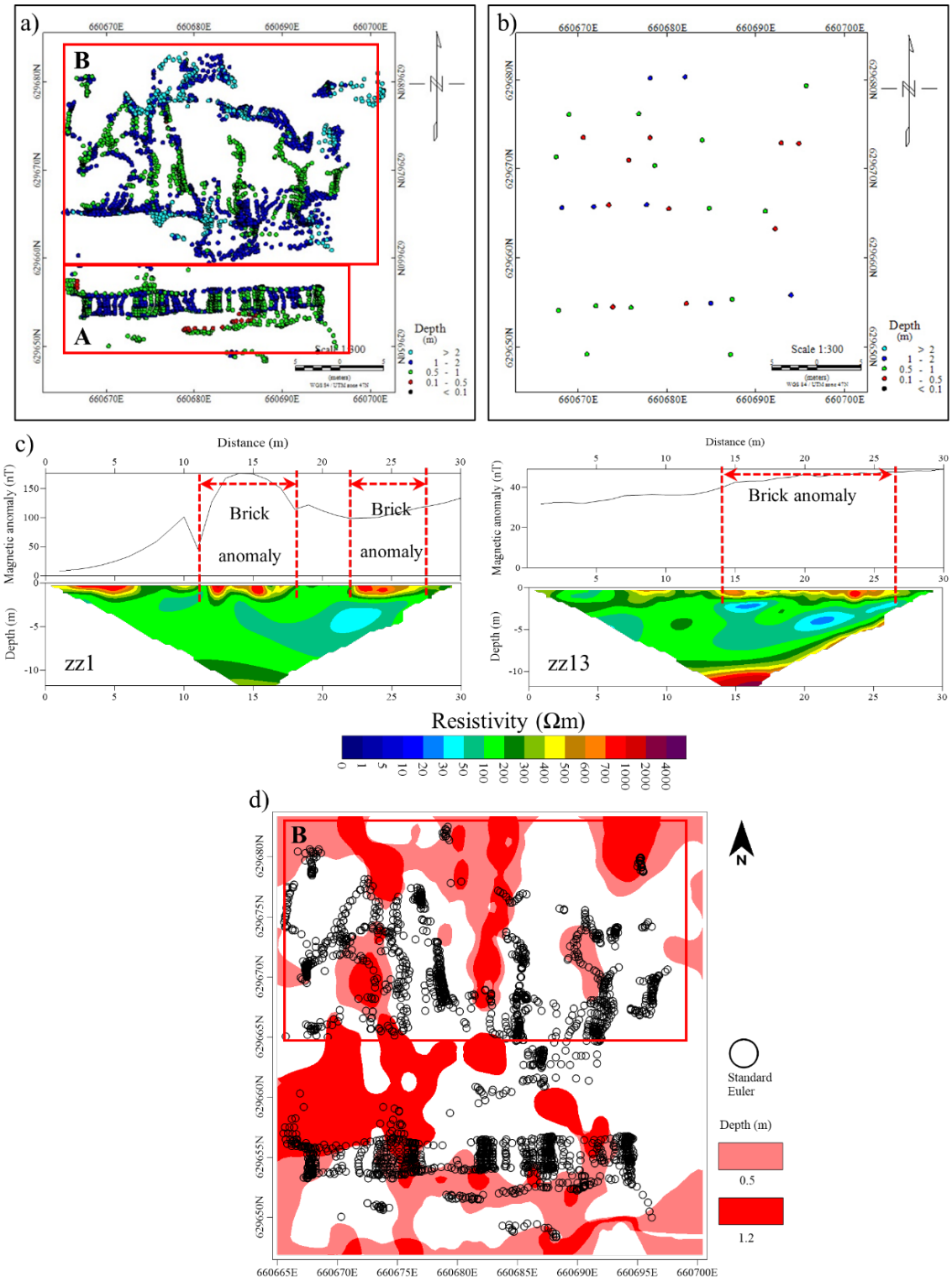

FIGURE 8. a) Standard Euler deconvolution map, b) Located Euler deconvolution map, c) Integrated magnetic anomaly with 2-D resistivity model for zz1 and zz13, and d) Brick-clay resistivity anomaly distribution with integrated Euler map

correlated with the edges of the resistivity anomaly, which represents the floor and the wall of the structures.

Figure 9 presents the integration analysis of the SB2 study area. The plotted Euler map represents the lateral location depths of the causative sources of magnetic anomalies. The standard Euler (Figure 9(a)) map reflects numerous solutions which were concentrated along a specific trend. The map shows more features of the buried structures with a depth ranging from 0.1-2.0 m as distributed along the map. The map indicates that more solutions are concentrated in the western part. The features might be associated with the buried clay bricks, which refer to the floor or wall of the structures. The striking pattern concentrating at a depth of 0.5-1 m at the western part

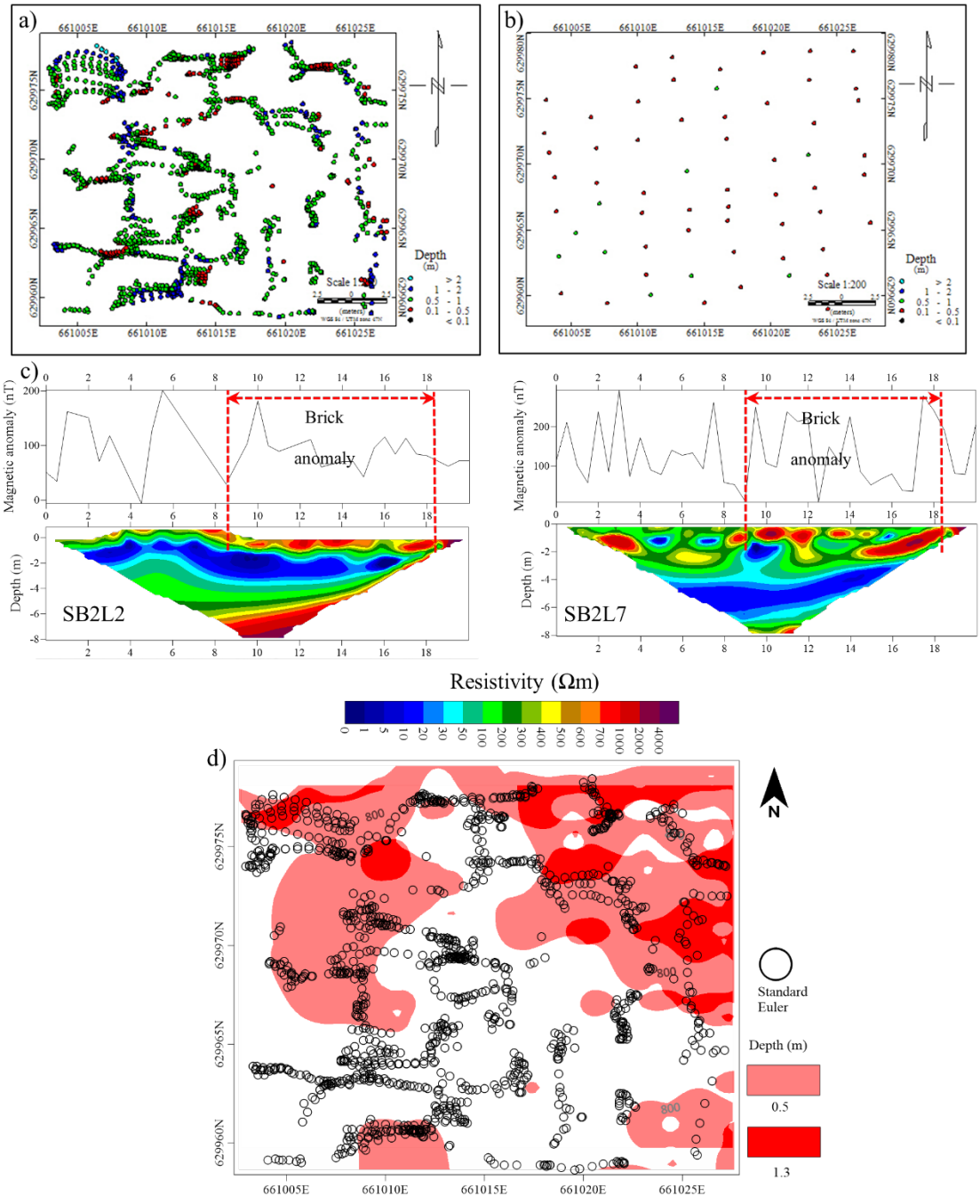

FIGURE 9. a) Standard Euler deconvolution map, b) Located Euler deconvolution map, c) Integrated magnetic anomaly with 2-D resistivity model for SBL2 and SBL7, and d) Brick-clay resistivity anomaly distribution with integrated Euler map

could refer to the collapse of the outer foundation, which covers the floor structures underneath at a depth >1 m. The eastern part of the map shows scattered red solutions and might be linked to the clay brick that dislocated from the original positions. Meanwhile, the located Euler (Figure 8(b)) depicts insignificant results as compared to the standard Euler.

The magnetic values showed the possibility of clay bricks distributions with values ranging from 50-140 nT while the 2D resistivity models show high resistivity values at ranges of 400-1000 Ωm at depth of ≤1.5 m. The results from the magnetic SB2L2 line, at a distance of 8.5 to 19 m demonstrated high magnetic values >50 nT, which correspond to high resistivity values of >400 Ωm. Magnetic and resistivity SB2L7 lines at a distance of 9 to 19 m show a high magnetic and resistivity with average values of >50 nT and >400 Ωm, respectively. The magnetic and 2-D resistivity results show a good correlation yielded the same interpretations representing the clay brick. The distribution of the anomaly from the resistivity correlated with the Euler deconvolution map as shown in Figure 9(d). The distribution of the Euler solution located at the edges of the anomaly might represent the buried structure of the clay brick. The resistivity anomaly was based on the contour values of 400 to 1000 Ωm with a depth of 0.5 and 1.2. Several Euler magnetic closures were observed that were not above the resistivity contour due to values <400 Ωm. The distribution of Euler magnetic with the resistivity anomaly represents the floor of the buried structure, which mainly covers the north-western and north-eastern of the map.

CONCLUSIONS

The integrated methods of magnetic and 2-D resistivity provide comprehensive subsurface images with corroboration of excavations data. The results validate the potential anomalies of the clay brick distributions. The success of these integrated methods is dependent on the contrast between geophysical parameters and environmental conditions. Although each method measures different physical characteristics, integrating their results demonstrates their ability to detect buried structures to some extent. The *in-situ* excavations on the SB2ZZ study area successfully validated the result and the interpretation of the geophysical survey. The information from the geophysical study would also indirectly reduce the number of pits and avoid unnecessary digging. The result from the excavation of the SB2ZZ area showed that the site once acted as a multi-functional building at the Sungai Batu complex. This area is significant due to the presence of large building structures that were constructed towards the ancient river. The suspected location of the potential archaeological area depicts identical characteristics such as a slightly raised mound with some exposed clay bricks on the surface, which exhibit high magnetic anomalies and resistivities ranging from 50 to 140 nT and 400 to 1000 Ωm, respectively. The extended processing of magnetic data includes the magnetic derivative derivation, analytic signal, and Euler deconvolution, as they all provide more detailed information regarding the clay brick distributions. The integrated map, comprising Euler deconvolution and resistivity values with specific depths, assists in elucidating the foundation of buried structure based on the trend and distribution of the anomalies. Conclusively, these methods offer valuable contributions to archaeological investigations by relying upon the presence of a physical contrast between the buried archaeological feature and the properties of the surrounding subsoil. The findings from the study area underscore the potential for this methodology to become a standard approach in similar archaeological contexts, particularly where structural remnants are expected or other unique environmental features. Future work in this area could focus on refining these methods for even greater resolution and accuracy in complex archaeological landscapes. For instance, the integration of advanced geophysical techniques, such as ground-penetrating radar (GPR) could offer complementary insights into stratigraphic layers and more complex structures. Additionally, enhancing data processing algorithms, such as by incorporating machine learning to identify subtle anomaly patterns, could lead to more precise interpretations of cultural layers and artifact distributions. Applying this integrated geophysical method across other sites within the Sungai Batu complex or similar ancient settlement areas could help build a more comprehensive understanding of historical construction practices, urban layouts, and even social organization patterns.

ACKNOWLEDGMENTS

The authors would like to thank Universiti Kebangsaan Malaysia (UKM) for Geran Galakan Penyelidik Muda with Project Code: GGPM-2023-042 entitle Integration of Geophysical Inversion for Heterogeneous Near-Subsurface Environments Using 2-D Cross-Plot Models. The authors thank the staff and postgraduate students from the geophysics program of the School of Physics, Universiti Sains Malaysia (USM) and the technical staff of the Centre for Global Archaeological Research (CGAR), Universiti Sains Malaysia (USM) for their assistance during data acquisition. The author wants to thank to Ms Nurina Auni Ismail for providing geophysical data as a part for her master's thesis.

REFERENCES

Ahmed, S.B., El Qassas, R.A. & El Salam, H.F.A. 2020. Mapping the possible buried archaeological targets using magnetic and ground penetrating radar data, Fayoum, Egypt. *The Egyptian Journal of Remote Sensing and Space Science* 23(3): 321-332.

Akca, İ., Balkaya, Ç., Pülz, A., Alanyalı, H.S. & Kaya, M.A. 2019. Integrated geophysical investigations to reconstruct the archaeological features in the episcopal district of Side (Antalya, Southern Turkey). *Journal of Applied Geophysics* 163: 22-30.

Allen, J. 2000. In support of trade: Coastal site location and environmental transformation in early historical period Malaysia and Thailand. *Bulletin Indo-Pacific Prehistory Association* 20: 62-78.

Ansari, A.H. & Alamdar, K. 2011. A new edge detection method based on the analytic signal of tilt angle (ASTA) for magnetic and gravity anomalies. *Iranian Journal of Science* 35(2): 81-88.

Aziz, A.M., Sauck, W.A., Shendi, E.A.H., Rashed, M.A. & Abd El-Maksoud, M. 2013. Application of analytic signal and Euler deconvolution in Archaeo-magnetic prospection for buried ruins at the ancient city of Pelusium, NW Sinai, Egypt: A case study. *Surveys in Geophysics* 34(4): 395-411.

Bevan, B.W. 1994. The magnetic anomaly of a brick foundation. *Archaeological Prospection* 1(2): 93-104.

FitzGerald, D., Reid, A. & McInerney, P. 2004. New discrimination techniques for Euler deconvolution. *Computers & Geosciences* 30(5): 461-469.

Hervé, G., Chauvin, A., Lanos, P., Rochette, P., Perrin, M. & Perron d'Arc, M. 2019. Cooling rate effect on thermoremanent magnetization in archaeological baked clays: An experimental study on modern bricks. *Geophysical Journal International* 217(2): 1413-1424.

Ihsan, S.R., Nordiana, M.M., Saad, R., Saidin, M., Maslinda, U., Hisham, H. & Sulaiman, N. 2015. Investigation of ancient river at Lembah Bujang, Kedah, Malaysia. *The Electronic Journal of Geotechnical Engineering* 20(11): 4385-4392.

Jeon, H.T., Hamm, S.Y., Lee, H.J., Park, S. & Kim, S.H. 2022. Delineating the Bonghwang earth castle and Royal Palace of Geumgwan Gaya Kingdom using multiple geophysical techniques. *Archaeological Prospection* 29(3): 465-478.

Khaw, N.R., Jun, G.L., Saidin, M.M., Mokhtar, N.A.M. & Abd Halim, M.H. 2021. The Sungai Batu archaeological complex: Re-assessing the emergence of ancient Kedah. *Kajian Malaysia: Journal of Malaysian Studies* 39(2): 117-152.

Khaw, N.B.R., Shahidan, S., Zainun, S. & Saidin, M. 2019. The post-14th century ancient Kedah: A port in decline? In *Role(s) and Relevance of Humanities for Sustainable Development*, *vol 68. European Proceedings of Social and Behavioural Sciences*, edited by Mat Akhir, N.S., Sulong, J., Wan Harun, M.A., Muhammad, S., Wei Lin, A.L., Low Abdullah, N.F. & Pourya, M. Asl. Future Academy. pp. 25-34. https://doi.org/10.15405/epsbs.2019.09.3

Milo, P., Vágner, M., Tencer, T. & Murín, I. 2022. Application of geophysical methods in archaeological survey of early medieval fortifications. *Remote Sensing* 14(10): 2471.

Mokhtar, N.A., Muztaza, N.M., Saidin, M., Saad, R., Masnan, S.S.K., Ismail, N.A., Bery, A.A., Jia, T.Y., Sapiai, S., Zakaria, M.T., Yunus, N., Muztaza, N.M. & Ismail, E.H. 2022. Geophysical approach for the ancient iron in Sungai Batu, Bujang Valley, Kedah, Malaysia. *Acta Geodynamica et Geomaterialia* 19(3): 201-217.

Mokhtar, N.A.M. & Saidin, M. 2018. Budaya material industri besi di Kompleks Sungai Batu, Lembah Bujang, Kedah. *Jurnal Arkeologi Malaysia* 31(2): 29-39.

Pánisová, J. & Pašteka, R. 2009. The use of microgravity technique in archaeology: A case study from the St. Nicolas Church in Pukanec, Slovakia. *Contributions to Geophysics and Geodesy* 39(3): 237-254.

Pickartz, N., Hofmann, R., Dreibrodt, S., Rassmann, K., Shatilo, L., Ohlrau, R., Wilken, D. & Rabbel, W. 2019. Deciphering archeological contexts from the magnetic map: Determination of daub distribution and mass of Chalcolithic house remains. *The Holocene* 29(10): 1637-1652.

Piro, S., Sambuelli, L., Godio, A. & Taormina, R., 2007. Beyond image analysis in processing archaeomagnetic geophysical data: Case studies of chamber tombs with dromos. *Near Surface Geophysics* 5(6): 405-414.

Plattner, A.M., Filoromo, S. & Blair, E.H. 2022. Multi-method geophysical investigation at Snow's Bend, a Mississippian platform mound. *Archaeological Prospection* 29(3): 343-351.

Rapi, R.W.M., Jusoh, A.F. & Saidin, M. 2020. Mineralogical and geochemical properties of bricks from Sungai Batu monuments. *Bulletin of the Geological Society of Malaysia* 69: 149-156.

Saidin, M., Abdullah, J., Osman, J. & Abdullah, A. 2011. Issues and problems of previous studies in the Bujang Valley and the discovery of Sungai Batu. In *Bujang Valley and Early Civilisations in Southeast Asia*, edited by Chia, S. & Andaya, B.W. Department of National Heritage, Ministry of Information, Communications and Culture. pp. 16-26.

Salvatore, P., Enrico, P., Daniela, Z. & Melda, K. 2019. Multimethodological approach to investigate urban and suburban archaeological sites. In *Innovation in Near-Surface Geophysics: Instrumentation, Application, and Data Processing Methods,* edited by Persico, R., Piro, S. & Linford, N. Elsevier. pp. 461-504.

Samsudin, A.R. & Hamzah, U. 1999. Geophysical measurements for archaeological investigation: Case studies in Malaysia. *Bulletin of the Geological Society of Malaysia* 43: 418-489.

Sapiai, S.M., Saad, R., Nawawi, M.N.M., Shyeh, S.K. & Saidin, M.M. 2010. Geophysical applications in mapping the subsurface structure of archaeological site at Lembah Bujang, Kedah, Malaysia. *AIP Conference Proceedings* 1250(1): 189-192.

Taqiuddin, Z.M., Rosli, S., Nordiana, M.M., Azwin, I.N. & Mokhtar, S. 2017. Utilizing of 2-D resistivity with geotechnical method for sediment mapping in Sungai Batu, Kedah. *AIP Conference Proceedings* 1861(1): 030048.

Tong, L.T., Lee, K.H., Yeh, C.K., Hwang, Y.T. & Chien, J.M., 2013. Geophysical study of the Peinan archaeological site, Taiwan. *Journal of Applied Geophysics* 89: 1-10.

USGS. 2022. *Shuttle Radar Topography Mission (SRTM) 1-Arc-Second Global*. US Geological Survey.

Vargemezis, G., Diamanti, N., Fikos, I., Stampolidis, A., Makedon, T. & Chatzigogos, N. 2013 Ground penetrating radar and electrical resistivity tomography for locating buried building foundations: A case study in the city centre of Thessaloniki, Greece. *Bulletin of the Geological Society of Greece* 47(3): 1355-1365.

Won, I.J. & Huang, H. 2004. Magnetometers and electromagnetomenters. *The Leading Edge* 23(5): 448-451.

Yordkayhun, S. 2021. Geophysical characterization of a sinkhole region: A study toward understanding geohazards in the karst geosites. *Sains Malaysiana* 50(7): 1871-1884.

Zakaria, I.I., Saidin, M. & Abdullah, J. 2011. Ancient jetty at Sungai Batu Complex, Bujang Valley, Kedah. *Postgraduate Student Forum: Current Asian Anthropology.* pp. 1-17.

*Corresponding author; email: taqiuddin@ukm.edu.my